Proceedings of PVP2003
2003 ASME Pressure Vessels and Piping Conference
July 20-24, 2003 Cleveland Ohio, USA

PVP2003-1958

MIXED MODE LOADING OF AN INTERFACE CRACK SUBJECTED TO CREEP CONDITIONS

Ali P. Gordon[1]
ag95@mail.gatech.edu
(404) 385-0279

David L. McDowell[1,2]
david.mcdowell@me.gatech.edu
(404) 894-5128

[1]**The George W. Woodruff School of Mechanical Engineering, Georgia Institute of Technology, Atlanta, GA 30332-0405 USA**
[2]**School of Materials Science and Engineering, Georgia Institute of Technology, Atlanta, GA 30332-0230 USA**

ABSTRACT

Interface cracks are seldom subjected to pure Mode I or pure Mode II conditions. Stationary interface cracks between two distinct, bonded elastic-creep materials subjected to remotely applied mixed mode loading are simulated. The finite element method (FEM) is used to examine crack tip fields and candidate driving force parameters for crack growth. Plane strain conditions are assumed. In most cases a functionally graded transition layer is included between the two materials. Examples of such systems include weld metal (WM) and base metal (BM) interfaces in welded or repaired boiler components subjected to elevated temperatures. Numerical solutions based on the asymptotic fields of the homogeneous and heterogeneous Arcan-type specimens are presented. Creep ductility-based damage models are used to predict the initial crack propagation trajectory. The incorporation of functionally graded transition layer regions affects the evolution of time-dependent stress components in the vicinity of the crack tip. The magnitude and direction of crack tip propagation can then be optimized with respect to interface properties.

KEYWORDS: Creep, functionally graded materials, bimaterials, finite elements, interfaces, mode mixity.

INTRODUCTION

Structures bonded via high temperature fusion processes are known as weldments. Examples are seam-welded pipes used in power generation equipment. The strengths of these structures are optimizing by manipulating the properties of the fusion zone. For example, by uniformly heating surfaces prior to the fusion process, formation of crack-like flaws and residual stresses upon cooling are reduced, thereby enhancing the structures fracture resistance. Reheating and annealing processes have been incorporated to minimize the microstructural variation, and subsequent variability of creep crack growth (CCG) behavior, among structured interfaces.

Research on bonded materials has evolved from studies that sought to introduce life-assessment techniques for in-service structures. For example, Saxena and others [1-4] obtained the creep crack growth (CCG) rates for overmatched WM and WM-BM CrMoV specimens machined from ex-service steam pipe sections. For small loads, the CCG rates for fused materials were consistently greater than those of homogeneous WM; however, large variability in the fracture toughness has also been observed. Experiments involving elastic-plastic interfaces show that the crack is likely to extend into the more plastic strain compliant material [5-7], thus leading to crack kinking. This further motivated the need to understand the crack tip driving forces at the interface. Shih and others [8-11] had previously addressed this problem by analyzing the asymptotic fields along interfaces in weldment models subjected to remote Mode I loading. Results predict crack kinking in the direction of the neighboring material that is more inelastically strain compliant.

The prediction of initial CCG rates were later related to microstructural mechanisms using physically-based creep damage models. Luo and Aoki [12] predicted fracture toughness of ductile interfaces using a modified Gurson [13] model to estimate void volume growth and link-up based on angular distributions of the hydrostatic and effective stresses. Segle and coworkers [14] used a modified Rice-Tracey (R-T) model [15] to predict initial void nucleation and coalescence along the interface, while Biner [16] predicted the crack growth rates in a similar fashion via a coupled creep deformation and diffusion model developed by Tvergaard [17]. Each determined that the void growth rates along the interface were much higher when the discrepancy between material properties of neighboring regions was larger. We extend these methods to ascertain the influence of remotely applied mixed mode loading on timed-dependent crack tip stress fields and initial CCG rates.

NOMENCLATURE

β	= remote mode mixity (°)
χ	= mismatch parameter
δ_{ij}	= identity tensor
ε_{ij}	= strain tensor
$\bar{\varepsilon}$	= effective strain
ν	= Poisson's Ratio
σ_{ij}	= stress tensor (MPa)
σ'_{ij}	= stress deviator (MPa)

$\bar{\sigma}$ = effective stress (MPa)
σ_m = mean or hydrostatic stress (MPa)
θ = angle from crack tip (°)
ω = scalar-valued damage variable
A = Norton creep coefficient (MPa^{-n})
a = crack size (mm)
B = specimen depth (mm)
BM = base metal region
E = elastic modulus (MPa)
HAZ = heat-affected zone region
M = stress triaxiality ratio
n = Norton creep strain hardening exponent
P = applied load (N)
r = distance from the crack tip (mm)
R = void radius (mm)
t = transition layer thickness (mm)
W = specimen width (mm)
WM = weld metal region

MIXED MODE FRACTURE

Mixed mode crack-tip loading occurs under a variety of mechanical or thermal loading, and environmental conditions. Material heterogeneity in the vicinity of a stressed crack tip affects the extent of the crack tip sliding stresses. Thus it is reasonable to assume that when an interface crack is exposed to a combination of remote loading modes, the level of material mismatch significantly alters the magnitudes of shear stress, deformation, and direction of crack propagation. This concept is depicted in Fig. 1.

Several criteria predict the direction of crack growth based on the near-tip strain, strain, or energy fields. The ratio of mean (hydrostatic stress) to Mises effective stress, known as the stress triaxiality ratio, M, i.e.,

$$M = \frac{\sigma_m}{\bar{\sigma}} = \frac{\sigma_{kk}}{3\bar{\sigma}} \tag{1}$$

has been used to estimate the magnitude of void nucleation and growth in creep ductile homogeneous materials [13,15]. M is also the basis of the stress triaxiality criterion given to predict the direction of crack extension, which was developed by and has been applied by Kong et al. [18]. The crack extension angle predicted by the so-called M-criterion satisfies the following conditions:

$$\frac{\partial M}{\partial \theta} = 0 \quad \frac{\partial^2 M}{\partial \theta^2} < 0 \tag{2}$$

Based on the asymptotic fields, M has been determined for homogeneous and weldment models exposed to remote mixed mode loading conditions.

In the following sections, the numerical approach that was implemented to obtain initial CCG trajectories is discussed. Afterwards, observations based on results are given. This paper concludes with a discussion of techniques to be developed to determine long term CCG rates magnitude and direction predictions for cracked interface bodies with time-dependent properties.

NUMERICAL SIMULATIONS

Whereas most existing experimental and analytical results describing fracture parameters and interface crack tip stress, strain, and displacement fields are derived using Mode I models, e.g. the SEN or CT-type specimens, the Arcan-type mixed mode fracture model is used in the current investigation. This specimen and its load fixture, developed by Amstutz and coworkers [19] and James and Sutton [20], has a remote loading range from pure Mode I to pure Mode II conditions.

Figure 2 shows the finite element (FE) representation of the mixed mode fracture model. It consists of nearly 3,000, 3-noded elements that are highly-refined near the crack tip with the smallest element size being $r=2.5x10^{-4}mm$. For each of the presented results the specimen size is $W=25.4mm$, the crack size is $a=0.666mm$, and the thickness is $B=12.7mm$. A load of $P=5.6kN$ was applied at increments of $\beta=\pm 5°$ around the crack tip, shown in Fig. 1.

BIMATERIAL INTERFACES

Most bimaterial fracture models address two distinct perfectly-bonded, isotropic, homogeneous constituents, with the initial crack being coplanar with the interface. The numerical models employed in this study are extensions of those used for the homogeneous case with several modifications. In a typical weldment, models are composed of two bonded homogenous, isotropic materials, each occupying either the region above or below the crack plane; however, in cases featuring a heat-affected zone (HAZ), a graded transition layer is introduced in a region between the homogeneous WM and BM regions. Elastic-secondary creep behavior models are employed for all materials in this study. Slight variations of the inelastic properties of the parent material (BM) are assumed for the weld (WM), while the HAZ metal was modeled as a functionally graded material (FGM) with properties matching of WM and BM on its boundaries.

The elastic properties of each material in the structure are identical, and are thus called *elastically-matched*. Under multiaxial stress states and steady state creep conditions, the materials is assumed to follow Norton's creep law, i.e.,

$$\dot{\varepsilon}_{ij} = \frac{1+\nu}{E}\dot{\sigma}_{ij} - \frac{\nu}{E}\dot{\sigma}_{kk}\delta_{ij} + \frac{3}{2}A\bar{\sigma}^{n-1}\sigma'_{ij} \tag{3}$$

At ambient temperature, $T = 538°C$, the material constants for the BM resembled those of 2¼CrMoV, which are given as [16],

$$\begin{aligned} &E = 160GPa, \nu = 0.33 \\ &A = 2.0\times10^{-17} MPa^{-n} hr^{-1} \\ &n = 5.7 \end{aligned} \tag{4}$$

The material property mismatch, χ, is defined as the weld-to-base metal ratio of any material property, for example $\chi_A = A_{WM}/A_{BM} = 100$. In the cases presented, the WM is more strain compliant than the BM; we say in this case that the properties are *undermatched* in the sense of strength. The converse case is *overmatched*. Remote loading mixity is varied concurrently material property mismatch.

Visualizations of the crack tip stresses and creep strains were obtained for a variety of models. The creep strains

accumulated after 10^6 hours in homogeneous BM and bimaterial WM-BM models are illustrated in Fig. 2. The accumulated creep strain in homogeneous models was, for the most part, not largely affected by the angle of remote loading, β; however, in the weldment case, creep deformation responded to β. For positive mode mixity, the creep strains were enhanced, whereas for negative mode mixity, the creep strains were suppressed.

CREEP DAMAGE

In creep ductile materials subjected to steady state CCG conditions, void initiation and nucleation are the processes that lead to crack tip propagation. Ligaments between voids experience amplified stresses, and at a critical size they fracture, causing neighboring voids to coalesce with each other and the crack tip. The crack can be considered to have advanced. Equation (3) does not adequately model the area-reduction transverse to the applied loading axis, leading to gradual loss of stress-carrying ability within the process zones of these materials.

Gradual reduction of load carrying capability (e.g. tertiary creep) can be accomplished through scaling the stress terms in creep relations such as Norton's law for secondary creep. Damage incorporated into the secondary creep strain rate term was first considered by Kachanov [21], and given as

$$\dot{\varepsilon}_{ij}^{c} = \frac{3}{2} A \frac{\bar{\sigma}^{n-1}}{(1-\omega)^{n}} \sigma'_{ij} \tag{5}$$

where A and n are the creep strain coefficient and exponent, respectively. The scalar-valued damage parameter, ω, is a state-dependent variable ranging from *0* for an undamaged material to *1* at failure. When $\omega = 0$ Eq. (6) reduces to the Norton law. One relation describing its evolution is given by [21]

$$\dot{\omega} = \frac{M_\omega \sigma_r^{\chi}}{(1-\omega)^{\phi}} \tag{6}$$

Here, σ_r describes the triaxial stress state and is related to the principal stress, σ_1, and the Mises effective stress, $\bar{\sigma}$, by

$$\sigma_r = \alpha\sigma_1 + (1-\alpha)\bar{\sigma} \tag{7}$$

An alternate form of the triaxial stress which incorporates the mean stress as been presented by Hayhurst [22]. Remaining terms in Eqs. (5)-(7), namely A, n, α, χ, ϕ, and M_ω, are considered material properties. The constants are typically optimized to fit deformation versus time curves obtained under constant mechanical and thermal loads [23].

The Rice-Tracey (R-T) model for spherical void growth [15] is an alternate evolution relation for a scalar-valued damage parameter based on the local triaxial stress state, and is given as

$$\frac{dR}{R_0} = 0.322 e^{1.5M} d\bar{\varepsilon} \tag{8}$$

Here, R is the void radius, and R_0 is the initial void radius, and $\bar{\varepsilon}$ is the effective total strain. The stress amplification due caused by area-reduction is $(1-R/\lambda)$, where λ is the void spacing. Cretegny [3] has determined R_0 and λ to estimate the remaining life in repaired turbine components. The stress triaxiality, M, is the ratio of mean and effective stresses given in Eq. (1).

Elastic-matching results in symmetric and smooth crack tip stress fields in all pure Mode I cases. In the homogeneous case, in which the specimen is entirely composed of BM, M remains constant from the iitial to the final times of load application time, t_o and t_f, respectively; however, in the bimaterial case, the steady state effective stress evolution is non-symmetric across the interface due to the inelastic property mismatch and near-tip shear stresses that exist near the crack plane. Upon initial loading, M is maximum in the direction that is transverse to the remotely applied load, β; however, as creep deformation occurs the maximum stress triaxiality occurs within the more strain compliant material, as shown in Fig 3. M is also affected by the remote mode mixity. At distinct locations around the crack tip, near θ=10° and 45°, M increases significantly with small changes of β.

FUNCTIONALLY GRADED INTERFACES

For the purpose of eliminating the complex, oscillatory crack tip behavior of elastic bimaterials, Atkinson was the first to introduce diffuse and graded interfaces [24]. This approximate representation is naturally occurring since most interfaces are diffuse over some length scale. Recent interfacial fracture mechanics research has incorporated material property gradation as a model variable [25-27]. Each applied spatially-dependent property variation to inelastic behavior. One that used a probabilistic approach to predict the fracture toughness and kink angle in FGMs was conducted by Becker et al. [28]. The Ritchie-Knott-Rice (RKR) statistical model [29] was included in a parametric study of the fracture toughness and kinking direction of elastic-plastic models with gradation either parallel or transverse to the initial crack.

In weldments, grading of mechanical properties arises from the fusion process. Contact between the liquefied weld metal (WM) and the base metal (BM) causes partial melting of the BM. This back-welding of BM allows intermingling of the two materials, so as the melt cools, the grains coarsen. This process inherently creates a new material section known as the heat-affected zone (HAZ). The representative microstructure around the weld zone is illustrated in Fig. 4. The thickness, t, of this region is controlled by weld temperature, weld time, and other factors. For simplicity, models that incorporate this layer between the WM and BM assume homogeneity of the HAZ. To obtain the HAZ region properties, a quasi-'rule of mixtures' is applied using the neighboring WM and BM properties. In some situations, this assumption leads to an inadequate representation of the structure and its response.

Indentation profiles of welded specimens reveal that the variation in Vickers hardness changes nearly linearly between the BM and WM regions [3,30] of repaired CrMo¼V turbine casting specimens. Characteristic microhardness profiles of weldment interface regions, shown in Fig. 5, correlate to linear yield strength variation between regions; moreover, they can be combined with the Norton power law rules to indicate that the

strain-hardening coefficient varies exponentially across the HAZ. An ABAQUS® [31] User-Defined Field (USDFLD) subroutine was developed to prescribe state-independent mechanical properties to the elements based on location of the integration points relative to the global coordinate system and the material boundaries.

Graded members have stress concentrations that are dependent on material properties and HAZ thickness. Shbeeb and Binienda [32] noted that thicker graded sections result in dramatically lowered near tip sliding stresses. By increasing the sharpness of the material property gradient, the near tip shear stress increased.

The phenomenon was also observed when the interface is subjected to mixed mode conditions, shown in Figs. 6-9. As the thickness of the HAZ region, t/W, was increased, the angular distribution of the crack tip stresses and M showed less variation. Each were obtained at a distance of $r=0.08mm$ from the crack tip. Local crack tip mode triaxiality decreased when the WM-HAZ interface is further away from the initial crack plane. As a result, the near tip behavior resembled that of homogeneous crack tip conditions. Accordingly, as t/W decreased, the angular variation of M, increased; however, its maximum and minimum magnitudes were unchanged.

As for the case with perfect bimaterial models, the maximum triaxiality occurred within the more creep strain compliant material. Remote mode mixity, β, was determined to have a weak inlfuence on the maximum stress triaxiality. The location of the maximum triaxiality about the crack tip generally occurred at small positive values, e.g. θ=10°, for decreasing t/W.

CONCLUSIONS

In homogeneous, power law creeping materials, the estimated crack propagation trajectories are transverse to the maximum tensile load [33]. The level of contribution of the shear mode brings about creep strains much faster because of the strong influence of the deviatoric stress on the creep strain. By conducting a parametric study of stationary cracks subjected to non-linear and time-dependent material behavior, the influence of the asymptotic stress fields was obtained. Based on the stress triaxiality states, we have inferred the likely direction of creep crack bifurcation. This direction is in the more creep strain compliant material, i.e., the WM in undermatched cases.

Transition layers between bimaterials have been included in this work; it was demonstrated that the severity of the stress triaxiality surrounding the crack tip is reduced relative to the distinct bimaterial interface case. The predicted behavior begins to approximate homogeneous behavior of the base metal (BM) as the transition layer thickness increases.

This type of simulation is relevant to the incubation period and allows for the redistribution of stress and accumulation of creep strain near the crack tip. Correlations of crack tip mode mixity and stress triaxiality to crack propagation trajectories can only be confirmed and extended by performing growing crack analyses in connection with experiments.

ACKNOWLEDGMENTS

Ali P. Gordon acknowledges support of an ONR fellowship in conducting this research. David L. McDowell is grateful for the support of the Carter N. Paden, Jr. Distinguished Chair in Metals Processing.

REFERENCES

[1] Liaw, P. K., Saxena, A., and Schaefer, J. (1989). "Estimating Remaining Life of Elevated-Temperature Steam Pipes-Part I. Materials Properties." Engineering Fracture Mechanics **32**(5): 675-708.

[2] Adefris, N. (1993). Creep-Fatigue Crack Growth Behavior of 1Cr-1Mo-0.25V Rotor Steel. Atlanta, GA, Georgia Institute of Technology.

[3] Cretegny, L. (1996). Fracture Toughness Behavior of Weldments at Elevated Temperature. Atlanta, GA, Georgia Institute of Technology.

[4] Saxena, A. (1998). Nonlinear Fracture Mechanics for Engineers. New York, CRC Press.

[5] Varias, A. G., Mastorakos, I., and Aifantis, E.C. (1999). "Numerical Simulation of Interface Crack in Thin Films." International Journal of Fracture **98**(3): 197-207.

[6] Shukla, A. (2001). "High-Speed Fracture Studies on Bimaterial Interfaces Using Photoelasticity." Journal of Strain Analysis for Engineering Design **36**(2): 119-142.

[7] Sorensen, B. F., and Horsewell, A. (2001). "Crack Growth Along Interfaces in Porous Ceramic Layers." Journal of the American Ceramic Society **84**(9): 2051-2059.

[8] Shih, C. F., and Asaro, R. J. (1988). "Elastic-Plastic Analysis of Cracks on Bimaterial Interfaces: Part I-Small Scale Yielding." Journal of Applied Mechanics **55**(2): 299-316.

[9] Shih, C. F., Asaro, R. J. (1989). Journal of Applied Mechanics: 763-779.

[10] Shih, C. F., Asaro, R. J., and O'Dowd, N. P. (1991). "Elastic-Plastic Analysis of Cracks on Bimaterial Interfaces: Part III - Large Scale Yielding." Journal of Applied Mechanics **58**(2): 450-462.

[11] Shih, C. F., Asaro, R. J., and O'Dowd, N. P. (1993). "Elastic-Plastic Analysis of Cracks on Bimaterial Interfaces: Interfaces with Structure." Materials Science and Engineering A **162**: 175-192.

[12] Luo, X. F., and Aoki, S. (1992). "Crack Growth on Elastic-Plastic Bimaterial Interfaces." International Journal of Fracture **57**: 365-379.

[13] Gurson, A. L. (1977). "Continuum Theory of Ductile Rupture by Void Nucleation and Growth: Part 1 -- Yield Criteria and Flow Rules for Ductile Media." Journal of Engineering Materials and Technology **99**: 2-15.

[14] Segle, P., Andersson, P., and Samuelson, L. (1998). "A Parametric Study of Creep Crack Growth in Heterogeneous CT Specimens by Use of Finite Element Simulations." Materials at High Temperatures **15**(2): 63-68.

[15] Rice, J. R., and Tracey, D. M. (1969). "On the Ductile Enlargement of Voids in Triaxial Stress Fields." Journal of Mechanics and Physics of Solids **17**: 102-217.

[16] Biner, S. B. (1998). " Characteristics of Interface Cracks." Materials Science and Engineering A **244**: 233-249.

[17] Tvergaard, V. (1984). "On the Creep Constrained Diffusive Cavitation of Grain Boundary Facets." Journal of Mechanics and Physics of Solids **32**(5): 373-393.

[18] Kong, X. M., Schlüter, N., and Dahl, W. (1995). "Effect of Triaxial Stress on Mixed Mode Fracture." Engineering Fracture Mechanics **52**(2): 379-388.
[19] Amstutz, B. E., Sutton, M.A., and Dawicke, D.S. (1995). "Experimental Study of Mixed Mode I/II Stable Crack Growth in Thin 2024-T3 Aluminum." Fatigue and Fracture, ASTM STP 1256 **26**: 256-273.
[20] James, M. (1998). A Plane Stress Finite Element Model for Elastic-Plastic Mode I/II Crack Growth. Manhattan, KS, Kansas State.
[21] Kachanov, L. M. (1958). "Time to Rupture Process Under Creep Conditions." Izv. Akad. Nank. **8**: 26-31.
[22] Hayhurst, D. R. (1983). "On the Role of Continuum Damage on Structural Mechanics." Engineering Approaches to High Temperature Design: 85-176.
[23] Hyde, T. H., Sun, W., and Williams, J. A. (1999). "Creep Behaviour of Parent, Weld and HAZ Materials of New, Service-Aged, and Repaired ½Cr½Mo¼V: 2 ¼Cr1Mo Pipe Welds at 640°C." Materials at High Temperatures **16**(3): 117-129.
[24] Atkinson, C. (1977). "On Stress Singularities and Interfaces in Linear Elastic Fracture Mechanics." International Journal of Fracture **13**: 807-820.
[25] Delale, F., and Erdogan, F. (1988). "Interface Crack in Nonhomogeneous Elastic Medium." International Journal of Engineering Science **26**(6): 559-568.
[26] Ozturk, M., and Erdogan, F. (1993). "Antiplane Shear Crack Problem in Bonded Materials with a Graded Interfacial Zone." International Journal of Engineering Science **31**(12): 1641-1657.
[27] Shaw, L. L. (1998). "The Crack Driving Force of Functionally Graded Materials." Journal of Materials Science Letters **17**: 65-67.
[28] Becker, T. L., Cannon, R. M., and Ritchie, R. O. (1998). A Statistical RKR Fracture Model for the Brittle Fracture of Functionally Graded Materials. 5th International Symposium of Functionally Graded Materials, Dresden, Germany, Trans Tech Publications.
[29] Ritchie, R. O., Knott, J. F., and Rice, J. R. (1973). "On the Relationship Between Critical Tensile Stress and Fracture Toughness in Mild Steel." Journal of Mechanics and Physics of Solids **21**(6): 395-410.
[30] Saxena, A., Cretegny, L., Grover, P. S., and Norris, R. H. (1998). "Modeling of Fracture and Crack Growth in Welds Operating at Elevated Temperatures." Materials at High Temperatures **15**(3): 259-263.
[31] ABAQUS® (1999). ABAQUS® User's Manual v.5.8. Providence, RI, Hibbitt, Karlsson, and Sorensen, Inc.
[32] Shbeeb, N. I., and Binienda, W. K. (1999). "Analysis of an Interface Crack for a Functionally Graded Strip Sandwiched Between Two Homogeneous Layers of Finite Thickness." Engineering Fracture Mechanics **64**: 693-720.
[33] Brockenbrough, J. R., Shih, C. F., and Suresh, S. (1991). "Transient Crack-tip Fields for Mixed-mode Power Law Creep." International Journal of Fracture **49**: 177-202.

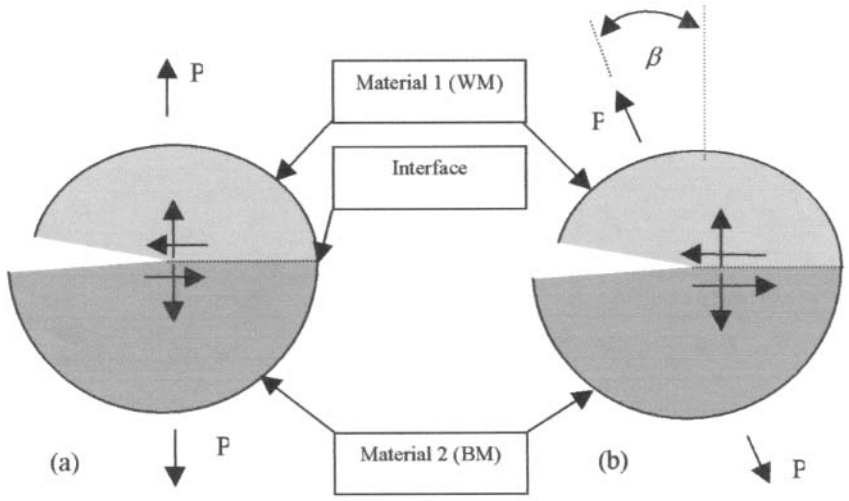

Figure 1: (a) An interface crack and (b) an interface crack that has kinked. Local crack tip mode mixity resulting from material strength mismatch is independent of remotely applied loading state.

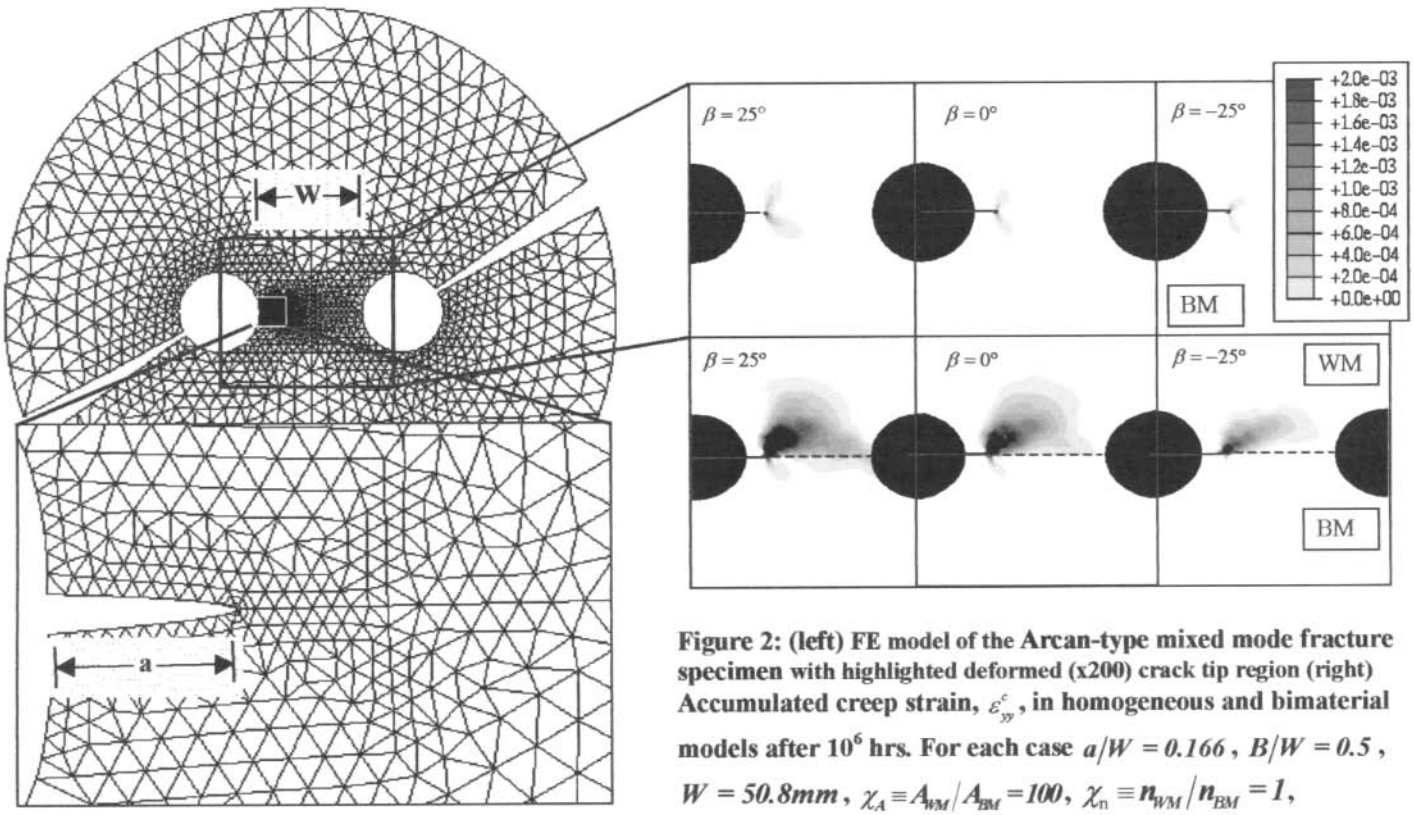

Figure 2: (left) FE model of the Arcan-type mixed mode fracture specimen with highlighted deformed (x200) crack tip region (right) Accumulated creep strain, ε^{c}_{yy}, in homogeneous and bimaterial models after 10^6 hrs. For each case $a/W = 0.166$, $B/W = 0.5$, $W = 50.8mm$, $\chi_A \equiv A_{WM}/A_{BM} = 100$, $\chi_n \equiv n_{WM}/n_{BM} = 1$, $T = 538°C$, and $P = 5.6kN$.

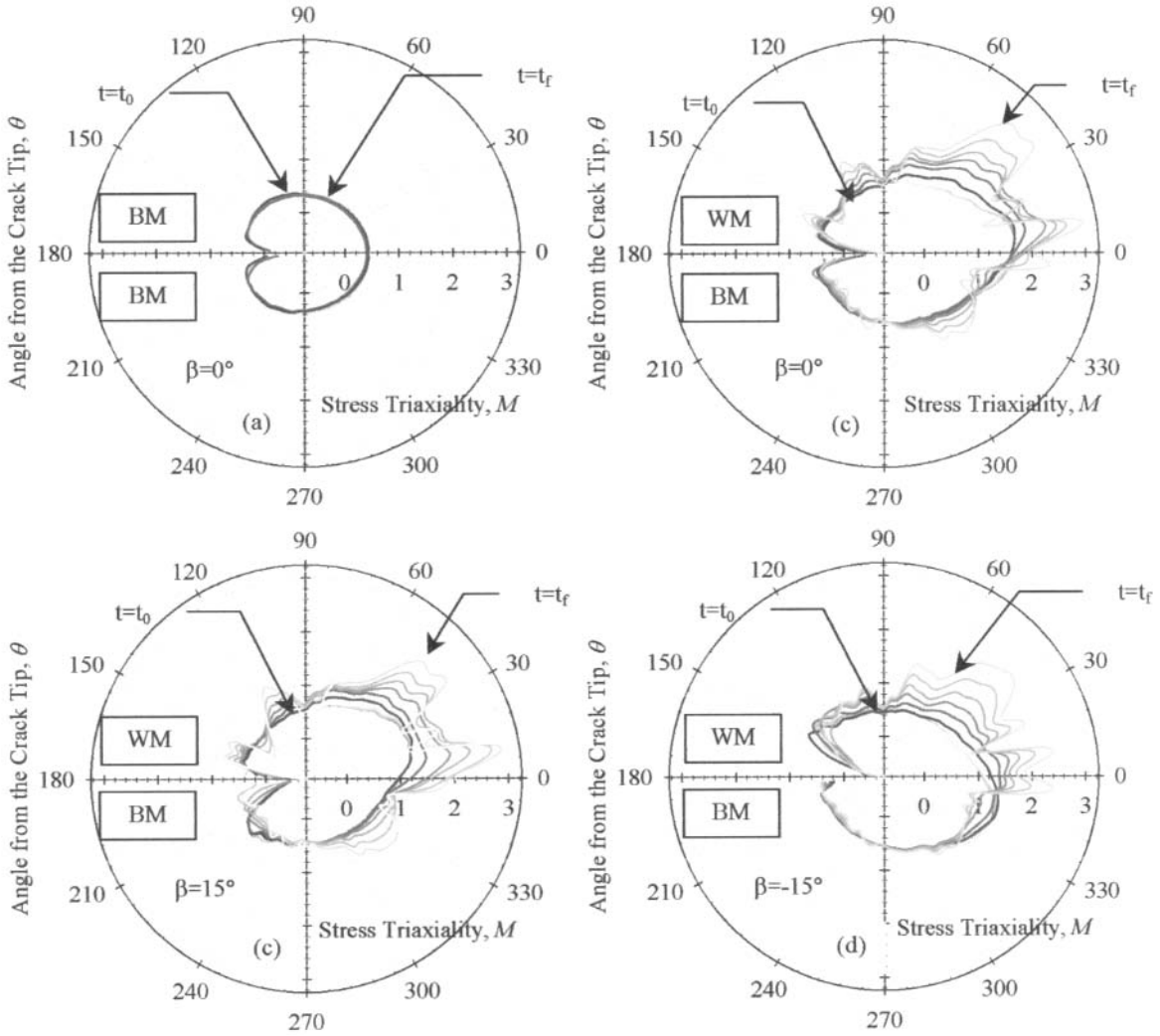

Figure 3: Time-dependent expansion of the angular distribution of the stress triaxiality, *M*, at a distance of *r=0.08mm* around the crack tip of bimaterial crack tips in elastic-creep materials. Models are exposed to remotely applied (a) Mode I ($\beta = 0°$) and (b,c) mixed mode loads ($\beta \neq 0°$). For each case $\chi_A=100$. The total exposure time was 10^6 hrs.

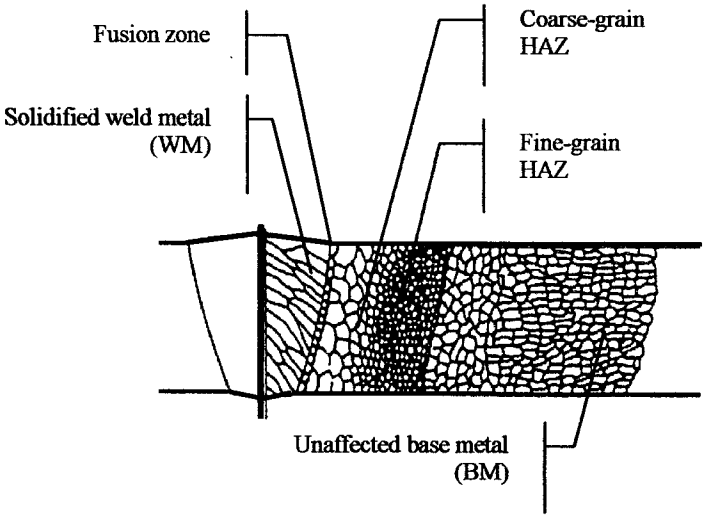

Figure 4: Representative microstructure surrounding the weld resulting from back-welding of the base metal (BM).

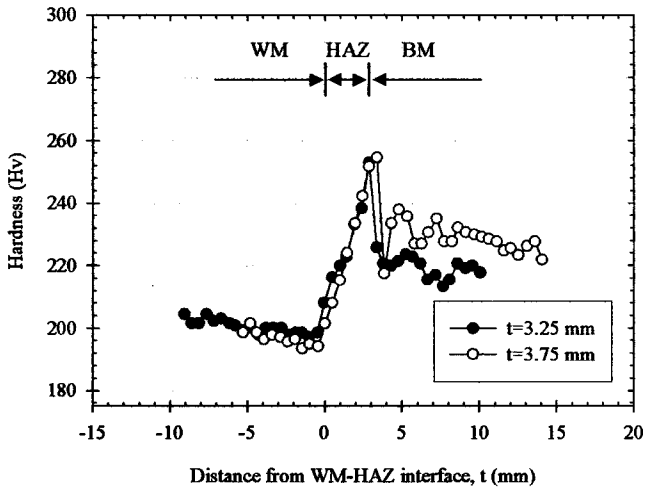

Figure 5: Microhardness identation profiles of welded structures with differing HAZ thicknesses.

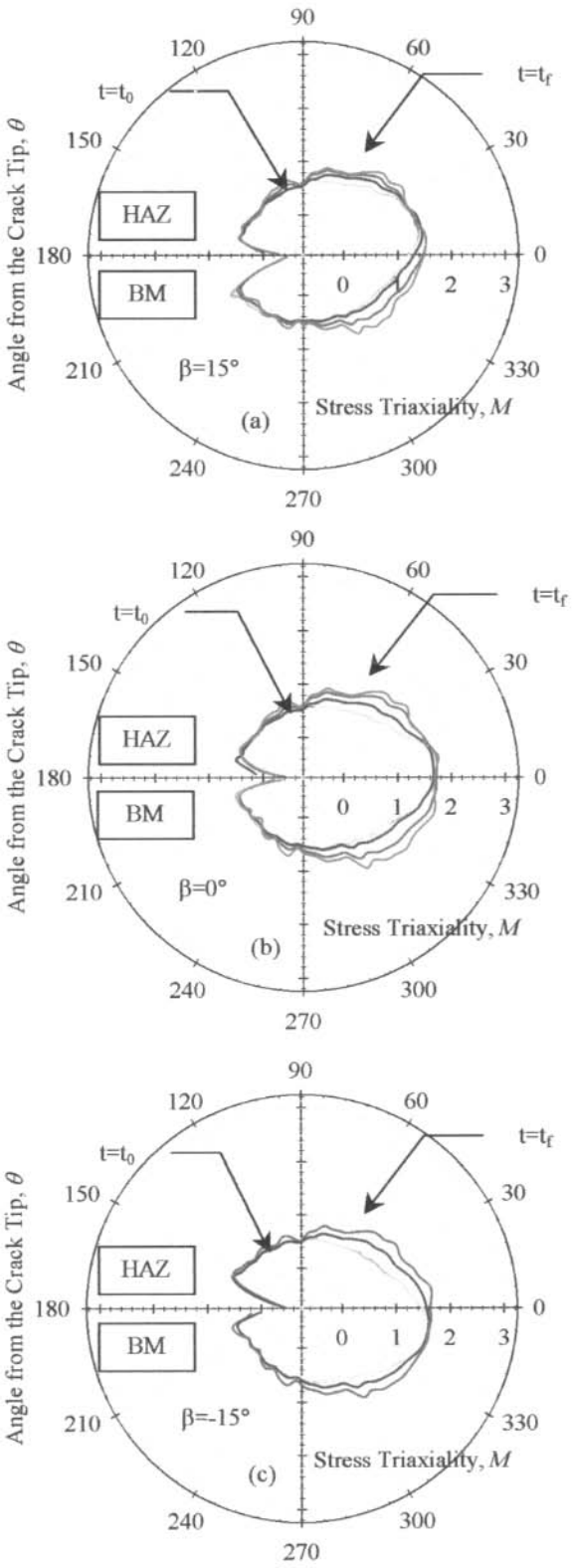

Figure 6: Time-dependent expansion of the angular distribution of the stress triaxiality, *M*, at a distance of *r=0.08mm* around the crack tip of bimaterial crack tips in elastic-creep materials. Models are exposed to remotely applied (a) Mode I (*β=0°*) and (b,c) mixed mode loads (*β≠0°*). For each case $\chi_A=100$ and $t_{HAZ}/W=0.833$. The total exposure time was 10^6

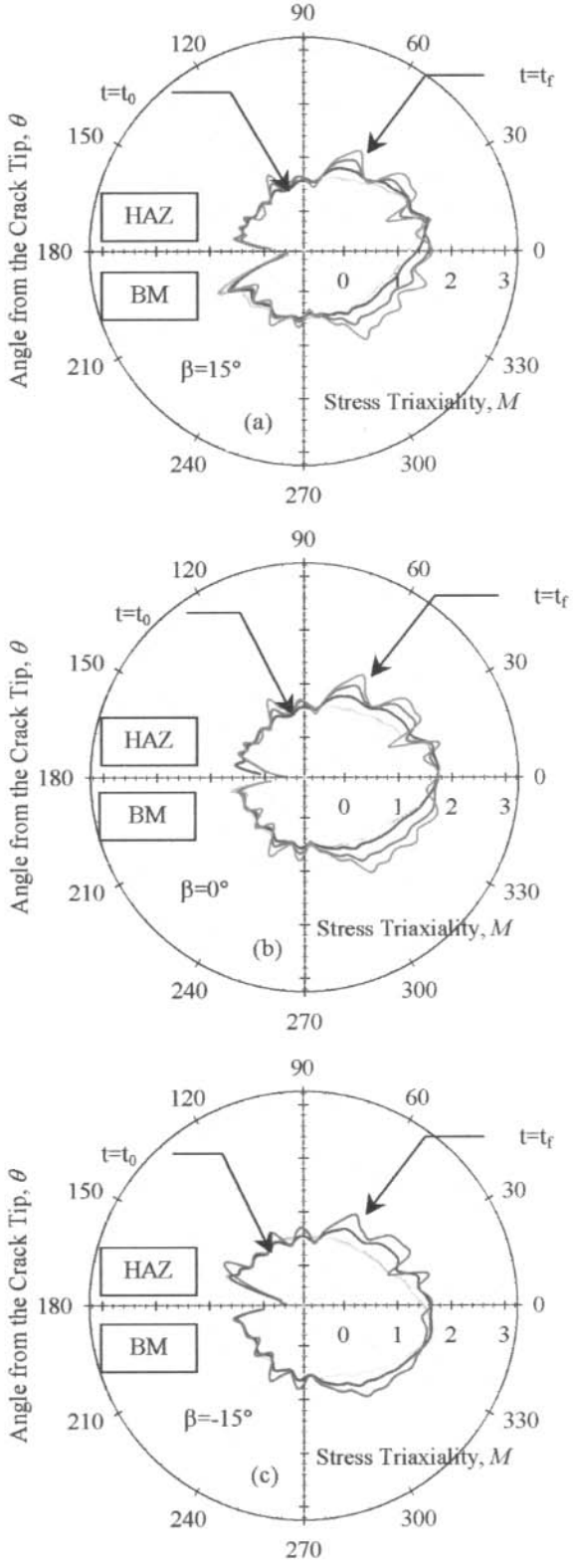

Figure 7: Time-dependent expansion of the angular distribution of the stress triaxiality, *M*, at a distance of *r=0.08mm* around the crack tip of bimaterial crack tips in elastic-creep materials. Models are exposed to remotely applied (a) Mode I (*β=0°*) and (b,c) mixed mode loads (*β≠0°*). For each case $\chi_A=100$ and $t_{HAZ}/W=0.5$.

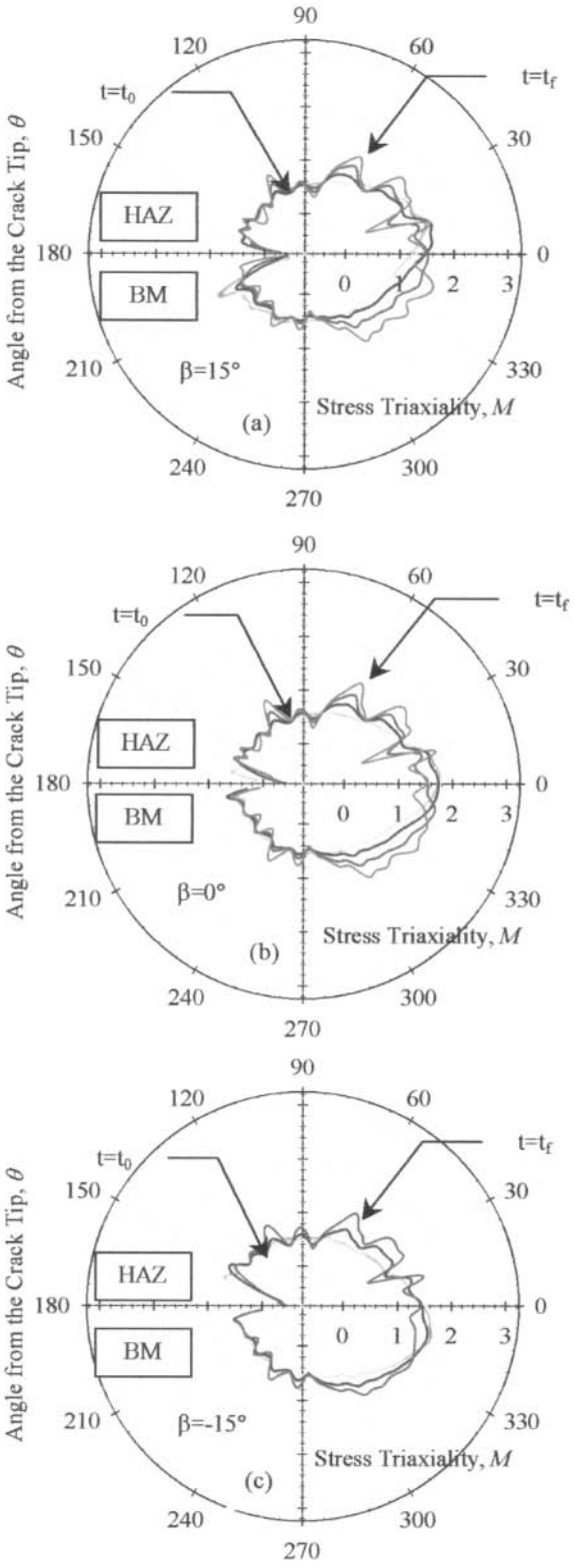

Figure 8: Time-dependent expansion of the angular distribution of the stress triaxiality, *M*, at a distance of *r=0.08mm* around the crack tip of bimaterial crack tips in elastic-creep materials. Models are exposed to remotely applied (a) Mode I (*β=0°*) and (b,c) mixed mode loads (*β≠0°*). For each case $\chi_A=100$ and $t_{HAZ}/W=0.25$. The total exposure time was 10^6

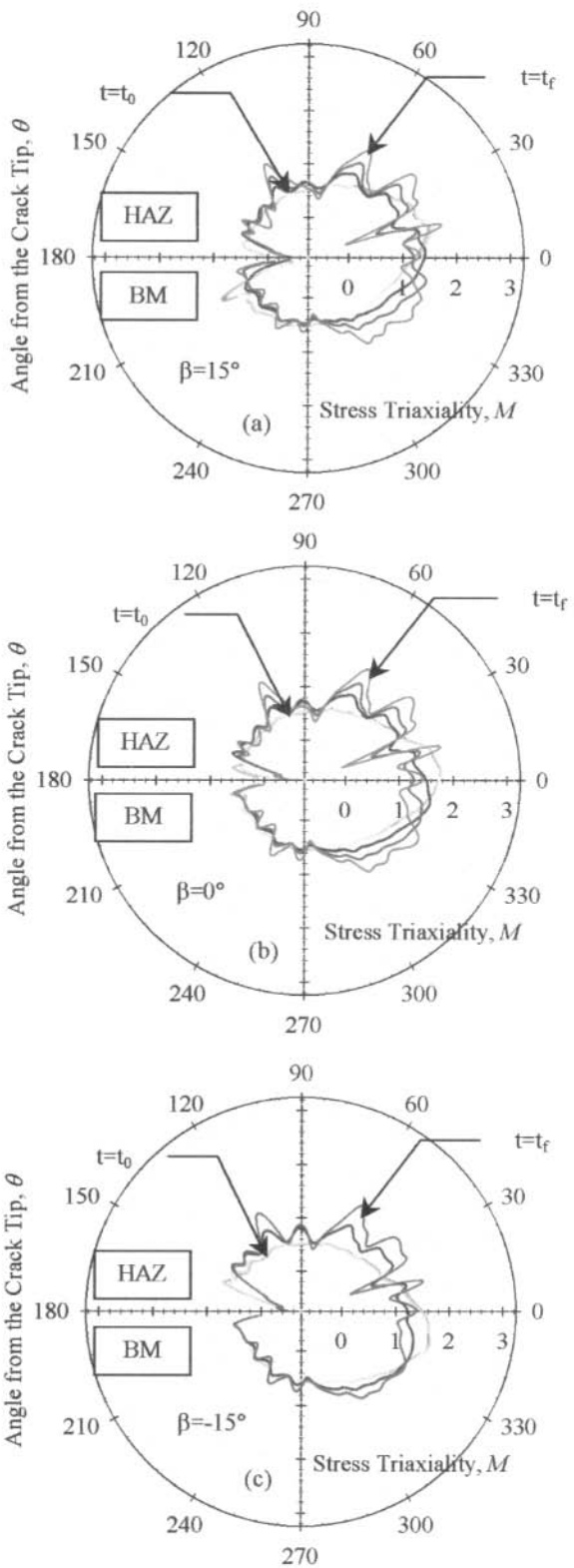

Figure 9: Time-dependent expansion of the angular distribution of the stress triaxiality, *M*, at a distance of *r=0.08mm* around the crack tip of bimaterial crack tips in elastic-creep materials. Models are exposed to remotely applied (a) Mode I (*β=0°*) and (b,c) mixed mode loads (*β≠0°*). For each case $\chi_A=100$ and $t_{HAZ}/W=0.125$. The total exposure time was 10^6